Electronic Supporting Information (ESI) for:

Projection method as a probe for multiplexing/demultiplexing of magnetically enriched biological tissues

*Mohammad Reza Zamani Kouhpanji and Bethanie J H Stadler **

M. R. Zamani Kouhpanji
Department of Electrical and Computer Engineering, Department of Biomedical Engineering, University of Minnesota Twin Cities, Minneapolis, USA.
200 Union SE St, 6-147C Keller Hall, Minneapolis, MN 55455.

B. J. H. Stadler
Department of Electrical and Computer Engineering, Department of Chemical Engineering and Materials Science, University of Minnesota Twin Cities, Minneapolis, USA.
200 Union SE St, 4-178 Keller Hall, Minneapolis, MN 55455.
Email: stadler (at) umn (dot) edu. Tel.: +1(612) 626-1628

Electrodeposition of magnetic nanowires (MNWs)

The nanowires were synthesized using the template-assisted electrodeposition technique, Figure ESI-1. The templates were porous polycarbonate sheets, Figure ESI-2. To make electrical contact, first 50nm layer of Ti was evaporated on one side of the templates as adhesion layer followed by a 300nm Au layer as conductive layer. The setup consists of three electrodes, where the template is located at the working electrode, Figure ESI-1. Other electrode is a Pt mesh (known as counter electrode) parallel to the working electrode to generate the electric field for depositing and the last electrode is a standard Ag/AgCl electrode as reference to control the current and voltage between the working electrode and counter electrode, Figure ESI-1. The electrolyte for each type of magnetic nanowires consists of different components as provided in the supplementary information. To grow the magnetic nanowires, an alternative voltage (-1.1V/-0.9V for 1sec/2sec) between the working electrode and the counter electrode was applied.

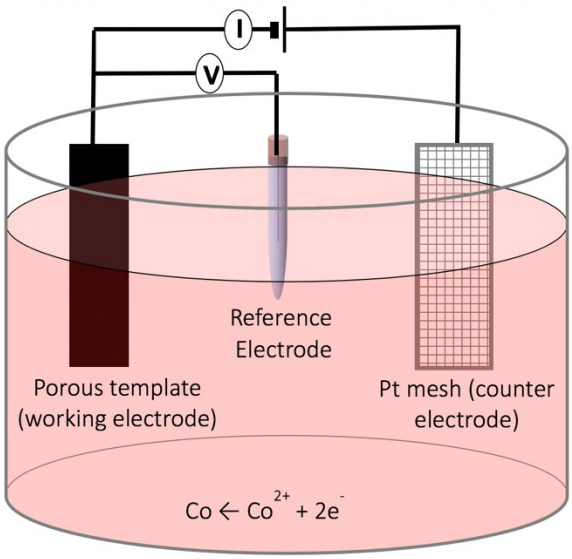

Figure ESI-1: A schematic of the three-electrode electrodeposition setup.

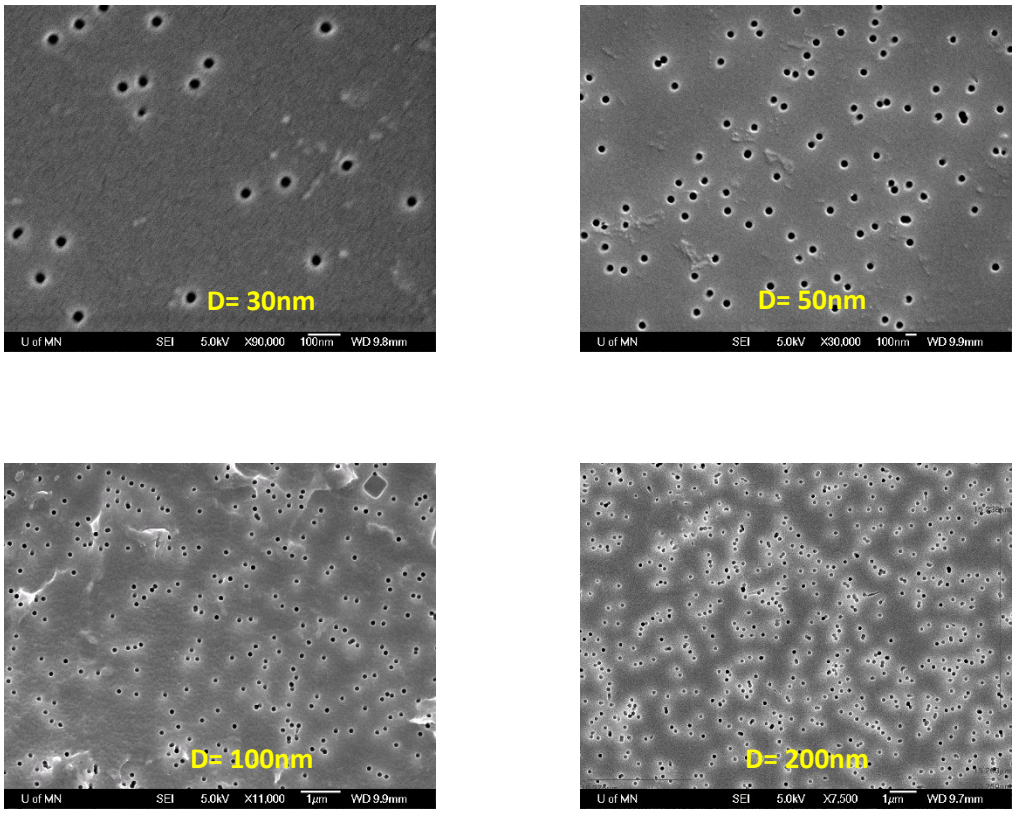

Figure ESI-2: The SEM images of the porous polycarbonate templates for synthesizing the magnetic nanowires.

All MNWs were electrodeposited into polycarbonate tissues with a broad range of diameters at room temperature, Figure ESI-2. The electrolyte for electrodeposition of cobalt (Co) consisted of boric acid (0.75 mole), cobalt sulfate (1.0 mole), and cobalt chloride (0.2 mole) at pH ~6.4. The electrolyte for electrodeposition of nickel (Ni) was composed of nickel sulfate (1 mole) and boric acid (0.5 mole) at pH ~3. Figure ESI-3 shows some SEM images of the MNWs.

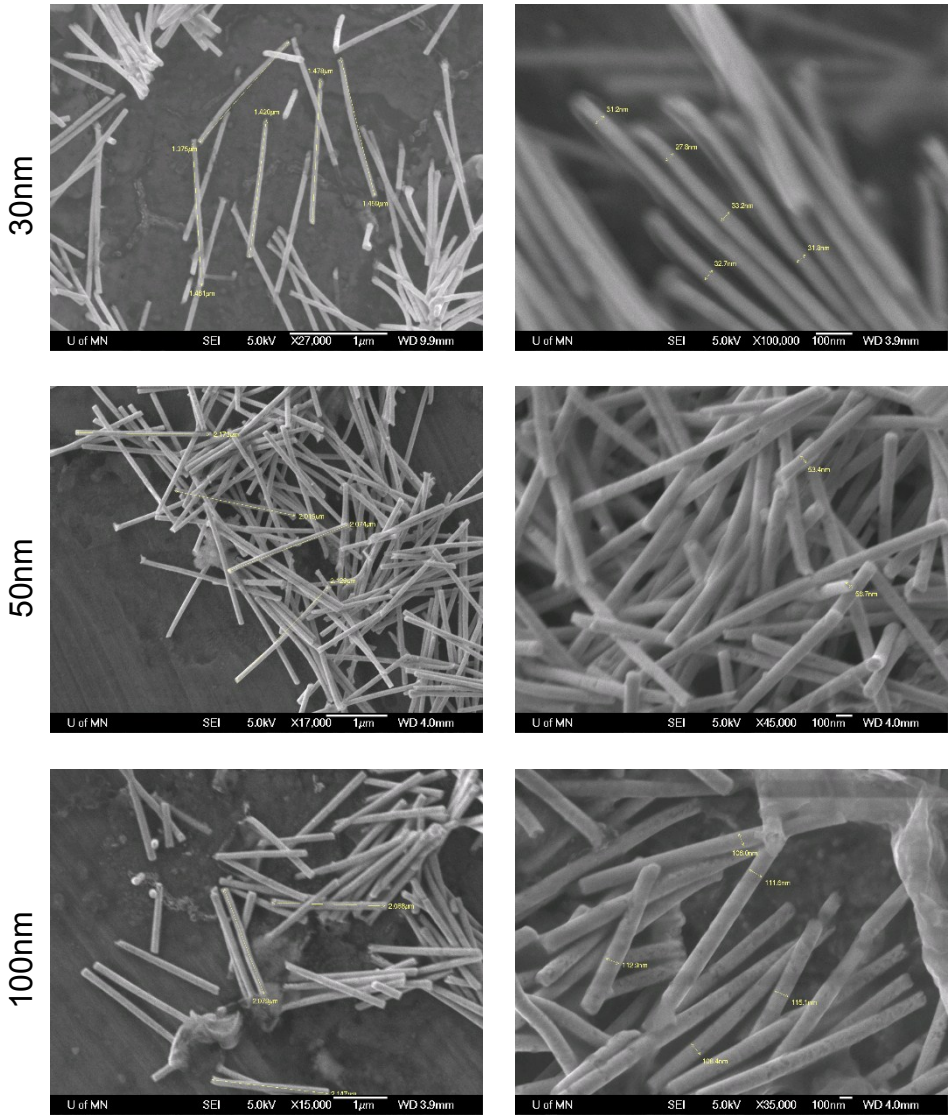

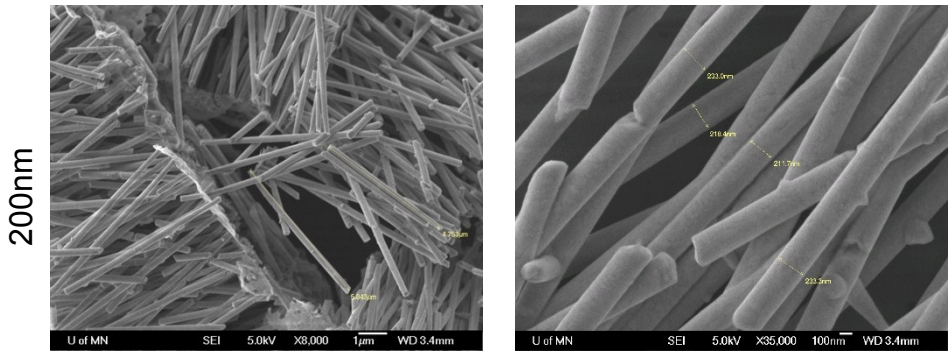

Figure ESI-3: The SEM images of polycarbonate templates and MNWs for structural characterization. The first column renders the diameter (pore size) for each row, the second and third columns are showing the images of the magnetic nanowires.

Theoretical origin of the projection method

Theoretically, each point inside the hysteresis loop indicates the presence of MNWs that switch during the application of H_b and H_f fields. Therefore, a probability density function can be introduced to determine the probability of finding a MNW switching in these particular fields. Mathematically, this is done by taking derivatives of the magnetization with respect to the H_b and H_f, similar to the Preisach distribution but in a tied region next to the upper branch of the hysteresis loop (UBHL). Thus, the probability of finding MNWs that switch in the region next to the UBHL is

$$P = -\frac{\partial^2 M}{\partial H_b \partial H_f} \tag{1}$$

For a deterministic quantification of the MNWs, one must take the integral from Eq. (1) to project out all MNWs that down-flip at H_b or up-flip at H_f. This results in two magnetic characteristics, where the down-flipping characteristic is

$$P_{H_b}(H_b) = \int_{H_b}^{\infty} \rho(H_b,H_f)dH_f = -\frac{\partial M(H_b,H_f)}{\partial H_b}\Big|_{H_f} \quad (2)$$

While the up-flipping characteristic is

$$P_{H_f}(H_f) = \int_{-\infty}^{H_f} \rho(H_b,H_f)dH_b = -\frac{\partial M(H_b,H_f)}{\partial H_f}\Big|_{H_b} = -RSF + \frac{\partial M_{lower}(H_f)}{\partial H_f} \quad (3)$$

To elaborate on the physical meaning of Eqs. (2) and (3), let us first look at the derivative of the UBHL in the context of the projection method

$$\frac{\partial M_{UBHL}(H_b)}{\partial H_b} = \frac{\partial M(H_f,H_b)}{\partial H_f})_{H_b=H_f} + \frac{\partial M(H_f,H_b)}{\partial H_b})_{H_b=H_f} = RSF \quad (4)$$

where, the first term is called the reversible switching field (RSF) because it determines the spontaneous magnetization change with the forward field; and the second term is called the irreversible switching field (ISF) because it determines the residual magnetization between two sequential backward fields at the same forward field.

Importantly, the down-flipping characteristic is the ISF and the up-flipping characteristic is the summation of the RSF and ISF, and they can be readily retrieved from the projection data, as shown in Figure 1 of the main text. Furthermore, because of the symmetry, the lower branch of the hysteresis loop is equivalent to the upper branch of the hysteresis loop.

The projection method data and statistical analysis

As explained in the main text, the projection measurements start by applying a large field to ensure the saturation of the sample. The field then is reduced to a backward field. Then the forward field is applied to return the field in the same field of the previous backward field while measuring the magnetization. Then the field should jump back to the saturation filed at one step to repeat the same process for the next backward fields. The solid black lines in Figure ESI-4 shows the data collected in this method, here we collected 5 data points from the backward field for better visualization.

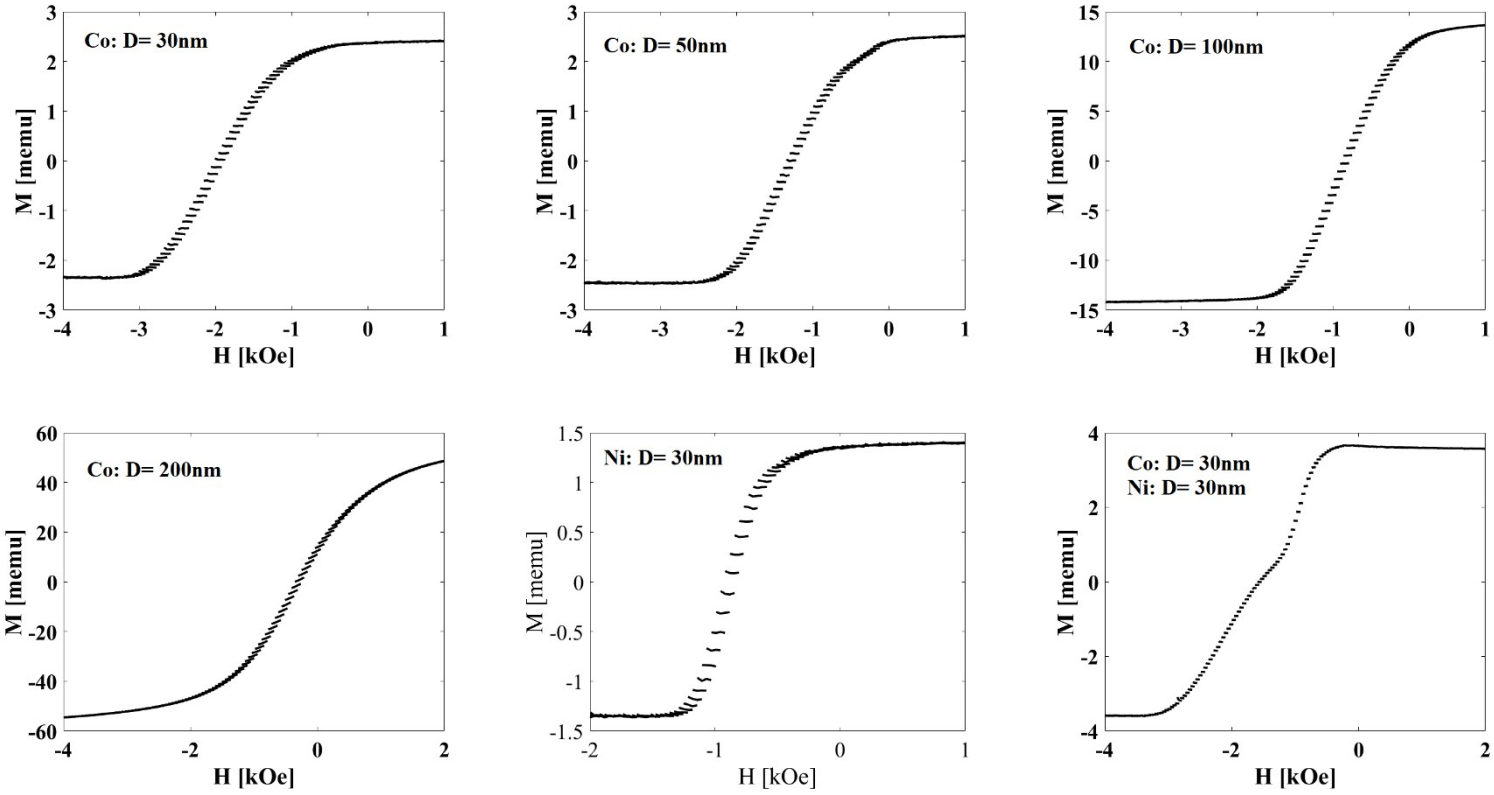

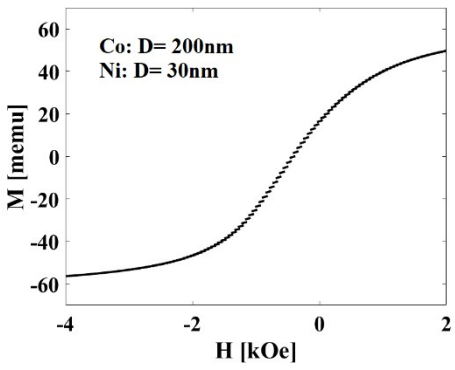
Co: D= 200nm
Ni: D= 30nm
M [memu]
H [kOe]

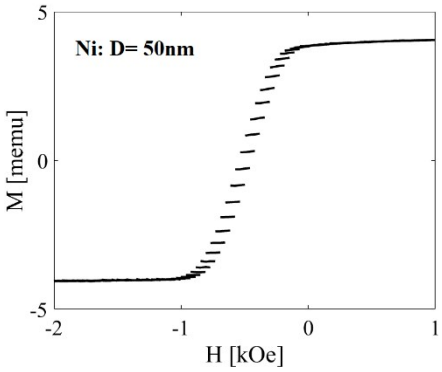
Ni: D= 50nm
M [memu]
H [kOe]

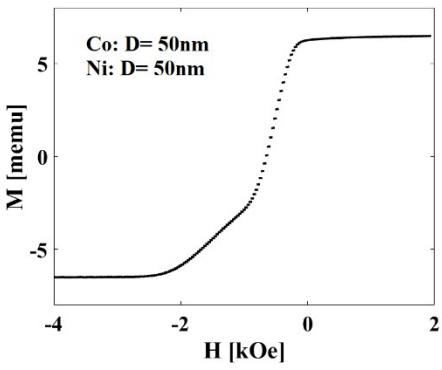
Co: D= 50nm
Ni: D= 50nm
M [memu]
H [kOe]

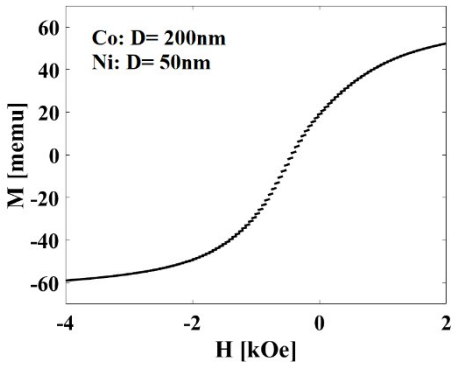
Co: D= 200nm
Ni: D= 50nm
M [memu]
H [kOe]

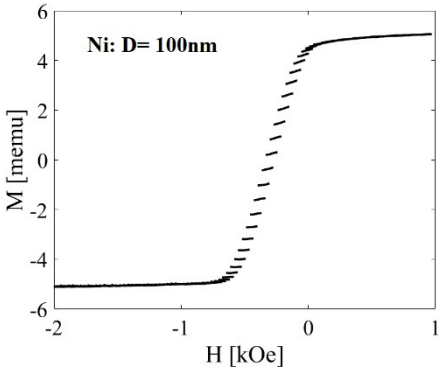
Ni: D= 100nm
M [memu]
H [kOe]

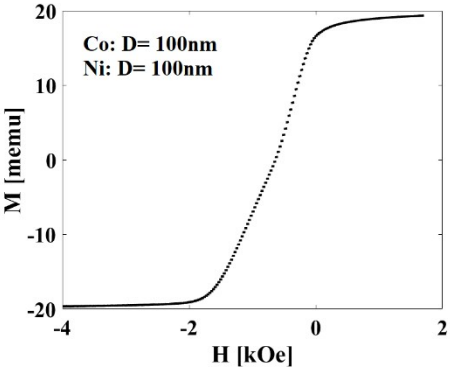
Co: D= 100nm
Ni: D= 100nm
M [memu]
H [kOe]

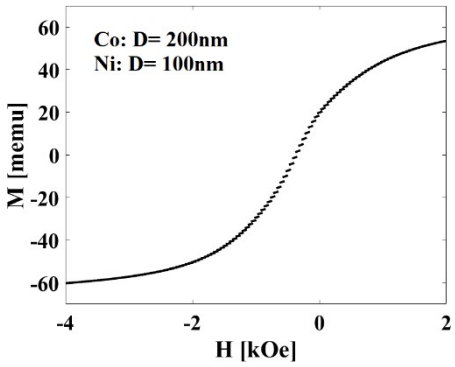
Co: D= 200nm
Ni: D= 100nm
M [memu]
H [kOe]

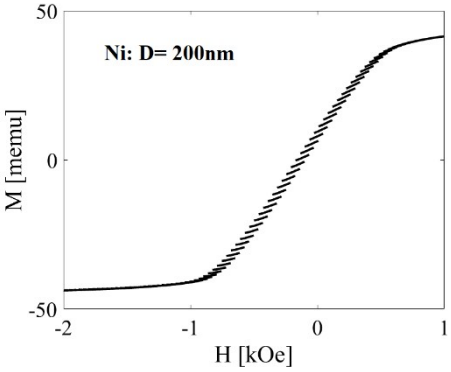
Ni: D= 200nm
M [memu]
H [kOe]

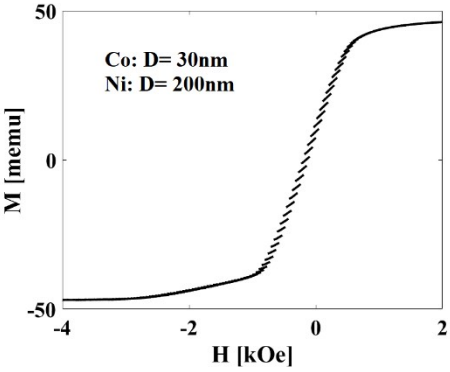
Co: D= 30nm
Ni: D= 200nm
M [memu]
H [kOe]

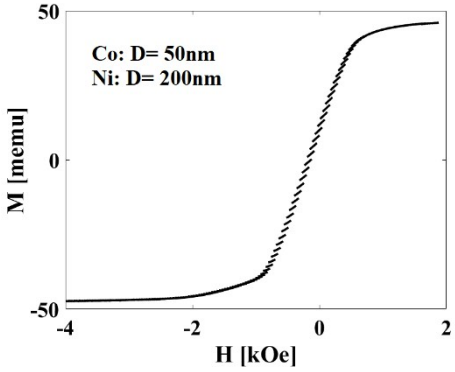
Co: D= 50nm
Ni: D= 200nm
M [memu]
H [kOe]

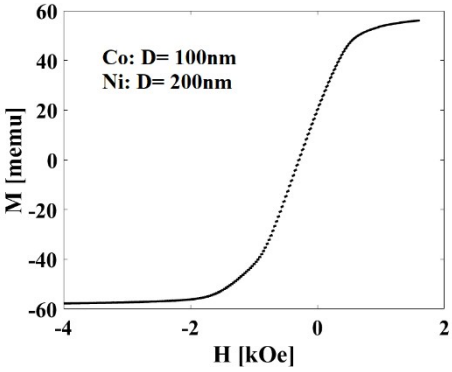
Co: D= 100nm
Ni: D= 200nm
M [memu]
H [kOe]

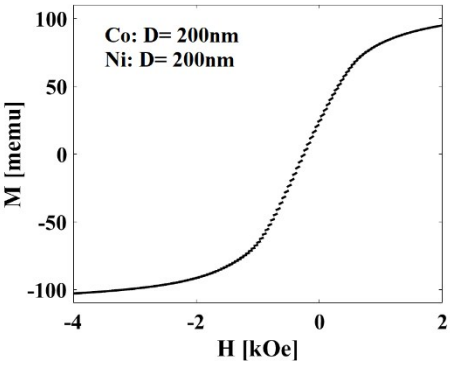
Co: D= 200nm
Ni: D= 200nm
M [memu]
H [kOe]

Figure ESI-4: the collected data using the projection method. The first five points were measured and shown for a better visualization even though the only the first two points are sufficient for determining P_{Hb}.

To find the volume ratio of each MNWs type in this combination, we wrote the "calibration curve" as follows (for example, let's consider P_{Hb} for Co and Ni with diameters of 30nm)

$$Calibration\ curve\ for\ P_{Hb} = \alpha_{Co:\,D=30nm} P_{HbCo:\,D=30nm} + \alpha_{Ni:} \quad (1)$$

where, *a* coefficients are the weight for each type. The RMS error is defined as

$$RMS = \sqrt{\frac{1}{N}\sum_{i=1}^{N}(Exp.\,data - Calibration\ curve)^2} \quad (2)$$

where, *N* is the number of data-points for the corresponding characteristic. The α coefficients are found while minimizing the RMS. Then, the volume ratio for *j* is calculated as follows

$$\chi_j = \frac{\alpha_j \times Vol_j}{\sum_{i=1}^{2} \alpha_i \times Vol_i} \times 100\ (\%) \quad (3)$$

where, Vol is the initial volume of each type that was added into the combination. According to Eq. (3), if all α are 1.0, then the fit volume ratio is similar to the known volume ratio for each type of the MNWs. The results for the volume ratios are given in Figure 3 of the main text. Noted, the same procedure can be expanded for combinations including several types of MNWs.

MNWs coercivity

Coercivity is the field in which the magnetization is zero. The coercivity of the MNWs can be determined using the location of the P_{Hb} peak. It also can be found by looking at the zero magnetization at the left side of the projection data (given in Figure ESI-4). Figure ESI-5 provides the coercivity of all our MNWs types. The MNWs with smaller diameters have larger coercivity compared to the MNWs with larger diameters.

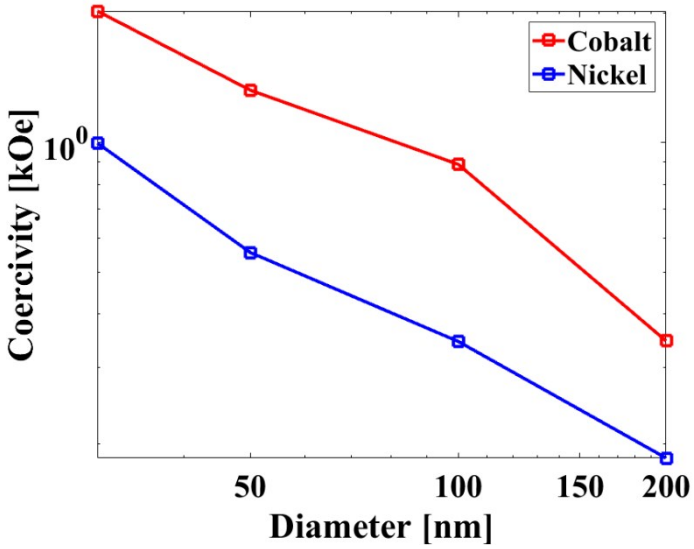

Figure ESI-5: The MNWs coercivity.